

A Differential Integrator with a Built-In High-Frequency Compensation

Mohamad Adnan Al-Alaoui, *Senior Member, IEEE*

Abstract—A novel integrator with differential inputs is described. The integrator uses a single RC network to control the integration action of the circuit. It performs at higher frequencies with higher quality factors than the traditional differential integrator. Simulation and experimental results support the theoretical derivations.

I. INTRODUCTION

THE differential integrator integrates the difference between its two input signals and is a basic component of active filters [1]. The traditional differential integrator uses two time constants [2]–[4]. The ability of the circuit to reject common mode signals depends, in addition to the CMRR of the amplifier, on the accurate matching of its two time constants [2], [3]. To avoid the problem of matching the two time constants, it is often found more convenient to use a two amplifier circuit with one amplifier acting as a simple inverter and the other as a summing integrator. Both of the above differential integrators require compensation at high frequencies [1], [4], [5]. The compensation methods depend on pole-zero cancellation. However, two obvious disadvantages of these methods are stated in [1], [5], and [6]. The first disadvantage is that the unity gain bandwidth varies among operational amplifiers and thus each amplifier should be compensated individually. In [6], the use of a potentiometer as a series resistance is suggested to overcome this disadvantage. The second disadvantage is that under changing ambient conditions, as explained in [1], [5], and [6], the compensation will no longer be satisfactory because they attempt to “match two electrically dissimilar elements to each other [5, p. 220].” Active compensation is employed to alleviate the disadvantages of passive compensation by utilizing “matching” operational amplifiers [1], [5], [6]. A disadvantage of the active compensation is that it would not work adequately if the operational amplifiers are not properly matched.

The approach in this paper extends the high-frequency range of the integrator without having the disadvantages of either the passive or the active compensation techniques. Indeed, the frequency range is limited, as will be shown, by the relation $\omega \ll 1/RC$ rad/s. It will be shown in Section II-B, that at high frequencies, the resulting transfer function could be obtained

by a pole-zero cancellation if $1/RC \gg \omega_c/2$, where ω_c is the unity gain bandwidth of the operational amplifier. The pole occurs, approximately, at the radian frequency which is equal to $[(1/RC) + (\omega_c/2)]$, and the zero occurs at the radian frequency which is equal to $1/RC$. This is quite different from trying to cancel out a pole at the unity gain bandwidth frequency of the operational amplifier, as the passive and active compensation schemes aspire to do. Thus, by choosing $1/RC \gg \omega_c/2$, we obtain an integrator limited by the higher dynamics of the operational amplifier and requiring neither the active compensation of “matching” operational amplifiers nor the passive compensation of “matching electrically dissimilar elements.” The usable high-frequency range of the integrator approaches the unity gain bandwidth of the operational amplifier.

The approach presented in this paper did not evolve from the view of compensating the Miller integrator, but rather from the idea of obtaining an integrator by inverting the traditional passive RC differentiator. In [7], the traditional approach to inverse system design was employed to design a noninverting integrator. In this paper, the approach is used to develop a differential integrator that extends the high-frequency range considerably beyond that of the Miller integrator. The resulting integrator has a built-in zero that could be used to control the frequency range of the integrator to achieve integrators with appropriately lower or higher frequency ranges than is possible by using the traditional integrators. Note that the resulting integrator frequency range will thus be limited at the upper end by the inverse of the RC time constant, i.e., $\omega \ll 1/RC$ radians/second, while for the traditional Miller integrator it is the lower frequency end that will be limited by the inverse of the RC time constant, i.e., $\omega \gg 1/A_o RC$, where A_o is the dc gain of the operational amplifier. Indeed very low-frequency integrators could easily be obtained by using the new approach. In addition, the resulting circuit acts as an amplifier for dc input voltages and thus exhibits a built-in low-frequency stability.

In [7], the addition of a second operational amplifier to be used as a buffer was suggested to avoid loading. The buffer may be dispensed with by proper loading. The proposed differential integrator dispenses with the buffer for high-frequency applications, by the proper choice of component values to avoid loading, and thus a single amplifier circuit is obtained. For a low-frequency integrator, a buffer may be used because its dynamics do not influence the operation of the integrator at low frequencies. Other proposed high-frequency integrators use multiple operational amplifiers [8].

Manuscript received February 17, 1997; revised August 27, 1997. This work was supported in part by the University Research Board of the American University of Beirut. This paper was recommended by Associate Editor A. Johns.

The author is with the Department of Electrical and Computer Engineering, American University of Beirut, Beirut, Lebanon.

Publisher Item Identifier S 1057-7122(98)02536-7.

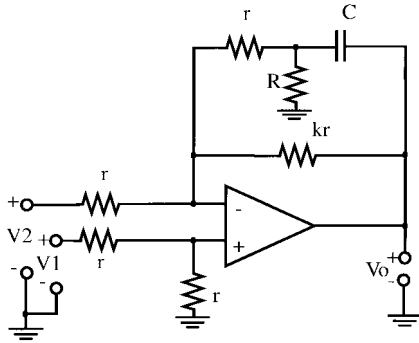


Fig. 1. The proposed differential integrator.

The proposed differential integrator has the advantages of a single time constant [3], dc stability [7], [9], and a built-in high-frequency compensation that extends the high-frequency range of operation [7].

II. THE PROPOSED INTEGRATOR

The proposed integrator is shown in Fig. 1. It is obtained by modifying the single input integrator developed in [7] and eliminating the buffer amplifier at high frequencies with appropriate loading conditions.

Nodal analysis of Fig. 1, similar to the analysis carried out in [7], and assuming that $r \gg R$, and that $k \gg 1$, yields

$$\frac{V_o}{V_1 - V_2} \approx \frac{1}{\frac{2}{A(s)} + \frac{RCs}{1 + RCs} + \frac{1}{k}} \quad (1)$$

The derivation of (1) is outlined in the Appendix. Note that the RC circuit should always be chosen so that it would act as a passive differentiator in the frequency range of interest, i.e., [7]

$$\omega \ll \frac{1}{RC}. \quad (2)$$

Equation (2) implies that $|RCs| \ll 1$ and that the RC product should be chosen appropriately for the frequency range of interest. Thus, the resistance and the capacitor should be chosen to give large RC product values for low-frequency integrators and should be chosen to give small RC product values for high-frequency integrators.

Thus, (1) may be simplified, using (2), to

$$\frac{V_o}{V_1 - V_2} \approx \frac{1}{\frac{2}{A(s)} + RCs + \frac{1}{k}} \quad (3)$$

A. The Ideal or Low-Frequency Case

Assuming $|A(s)| \gg k$, (3) reduces to

$$\frac{V_o}{V_1 - V_2} \approx \frac{k}{1 + kRCs}. \quad (4)$$

Equation (4), together with (2), represents an integrator for frequencies in the range

$$\frac{1}{kRC} \ll \omega \ll \frac{1}{RC}. \quad (5)$$

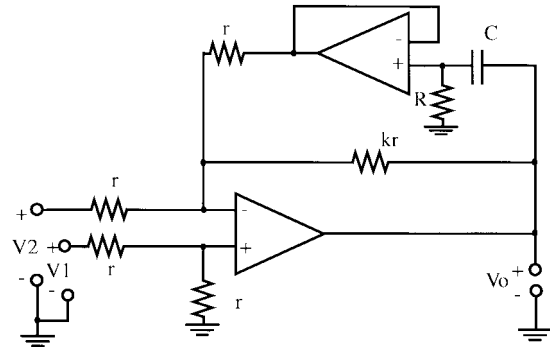


Fig. 2. The proposed low-frequency differential integrator with the additional buffer isolation amplifier.

The circuit acts as an amplifier for dc inputs. The dc gain is obtained from (1) by substituting the dc gain of the operational amplifier, A_o for $A(s)$ and zero for s in (1) to obtain $kA_o/(2k + A_o)$ which can be approximated as k for $k \ll A_o$, which in practice will always be satisfied. Thus the dc gain may be increased or decreased as desired by, respectively, increasing or decreasing k . Note that for low frequencies, the condition $R \ll r$ might entail using very large values of r . This could be mitigated by using a buffer isolation amplifier between r and R as shown in Fig. 2. The dynamics of the buffer amplifier do not influence the design at low frequencies.

B. The Nonideal Case

$A(s)$ may be approximated by a one-pole model and at high enough frequencies can be expressed as

$$A(s) \approx \frac{\omega_c}{s} \quad (6)$$

where ω_c is the unity gain bandwidth of the operational amplifier.

Substituting (6) into (3) yields

$$\frac{V_o}{V_1 - V_2} \approx \frac{k\omega_c}{\omega_c + (2k + kRC\omega_c)s}. \quad (7)$$

Equation (7) has a single pole that determines the start of the integration that is limited only by the higher order dynamics of the operational amplifier. The 3-dB frequency occurs at the pole and thus may be increased by decreasing k and/or decreasing the RC product. If k is chosen to satisfy a desired dc gain, then the 3-dB frequency may be increased by decreasing the value of the RC product. Note that the denominator of the Miller integrator is $s + [s + 1/(RC)]/A(s)$, and it is similar to the denominator of (3). However, substituting (6) in the denominator of the Miller integrator we obtain a second-order equation in s and the resulting transfer function has two poles. The first pole determines the start of the integration, while the second pole, that occurs at the radian frequency ω_c , causes the Miller integrator to quit at about $\omega_c/10$.

Equation (7), together with (2), represents an integrator in the frequency range

$$\frac{\omega_c}{k(2 + \omega_c RC)} \ll \omega \ll \frac{1}{RC}. \quad (8)$$

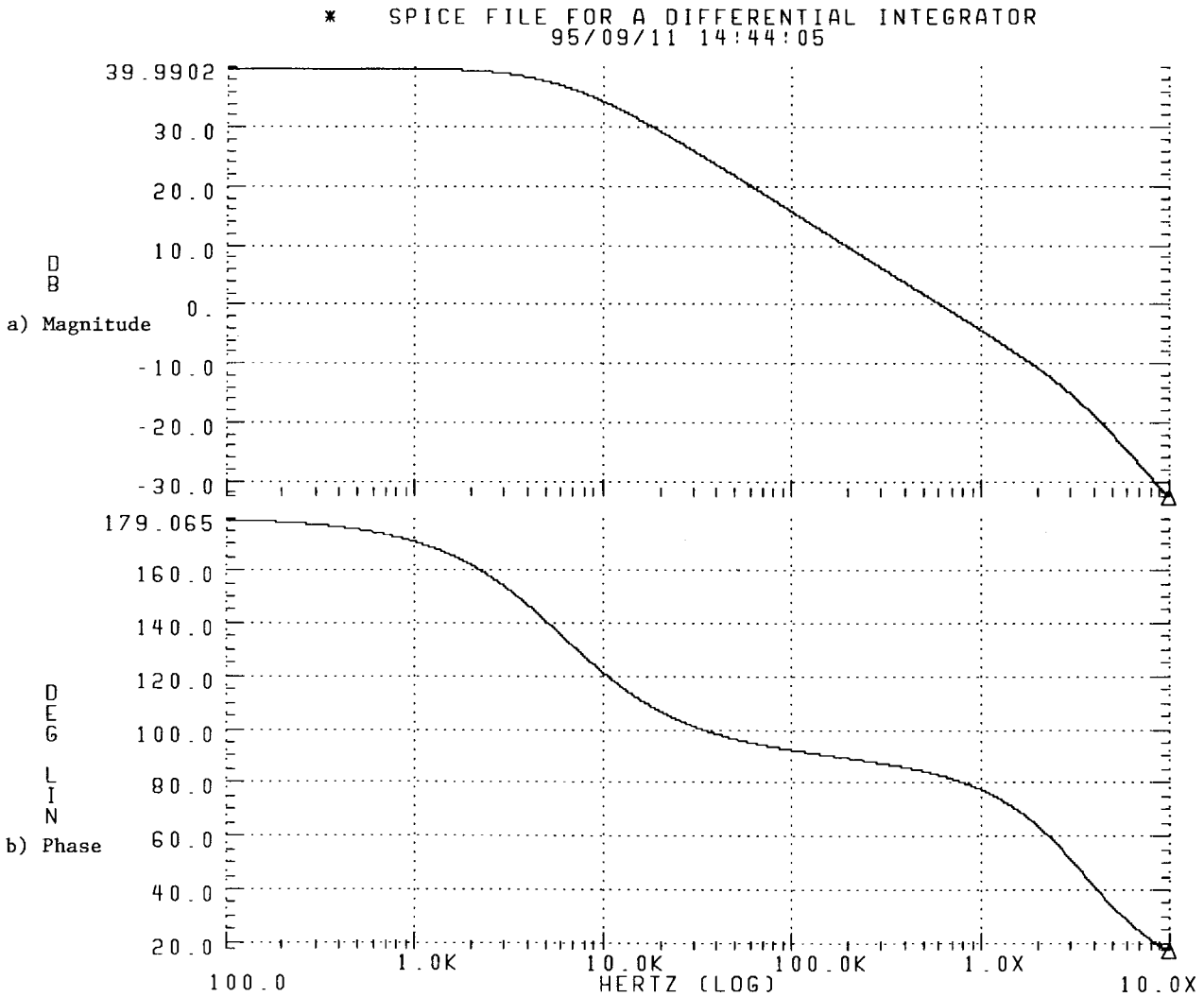


Fig. 3. HSPICE simulation of the integrator with the values of $r = 10 \text{ k}\Omega$, $k = 100$, $R = 500 \Omega$, $C = 100 \text{ pF}$, and LM741 operational amplifier. (a) The magnitude of the voltage transfer function in decibels and (b) the phase of the voltage transfer function in degrees.

For high frequencies, beyond one tenth of the unity gain bandwidth, and where the radian frequency ω is so close to ω_c such that $\omega_c RC \ll 2$, (9) simplifies to

$$\frac{\omega_c}{2k} \ll \omega \ll \frac{1}{RC}, \quad (9)$$

Substituting (6) into (1) yields

$$\frac{V_o}{V_1 - V_2} \approx \frac{\omega_c \left(s + \frac{1}{RC} \right)}{2 \left[s^2 + \left(\frac{1}{RC} + \frac{\omega_c}{2k} + \frac{\omega_c}{2} \right) s + \frac{\omega_c}{2kRC} \right]}. \quad (10)$$

Equation (8) is similar to the transfer function of the Miller integrator which was derived by Parrish and Allen in [10], except for the additional zero. This zero, if chosen properly, may reduce the excess phase due to the offending high-frequency poles and thus extend the high-frequency range of the integrator. It is to be noted that the second pole does not occur at ω_c , but is a function of ω_c and the RC product and occurs approximately at the radian frequency $[(1/RC) + \omega_c/2]$, as could be determined from the denominator of (10).

The second pole would occur at approximately $1/RC$ if we choose $1/RC \gg \omega_c/2$; then a pole-zero cancellation occurs in (10), and we obtain a single pole transfer function with the pole occurring at $\omega_c/2k$.

In contrast to active R integrators, both the lower and upper limits of the frequency range are controlled by the designer. In addition, the upper limit could be made greater than that possible in active R integrators. For example, the integrating summer reported in [11] yields a transfer function with a pole that limits the upper frequency range of the integrator.

III. THE INTEGRATOR QUALITY FACTOR Q

If we express the transfer function of an integrator as [7]

$$T(j\omega) = \frac{1}{R(\omega) + jX(\omega)} \quad (11)$$

then the Q -factor of the integrator is defined as

$$Q = \frac{X(\omega)}{R(\omega)}. \quad (12)$$

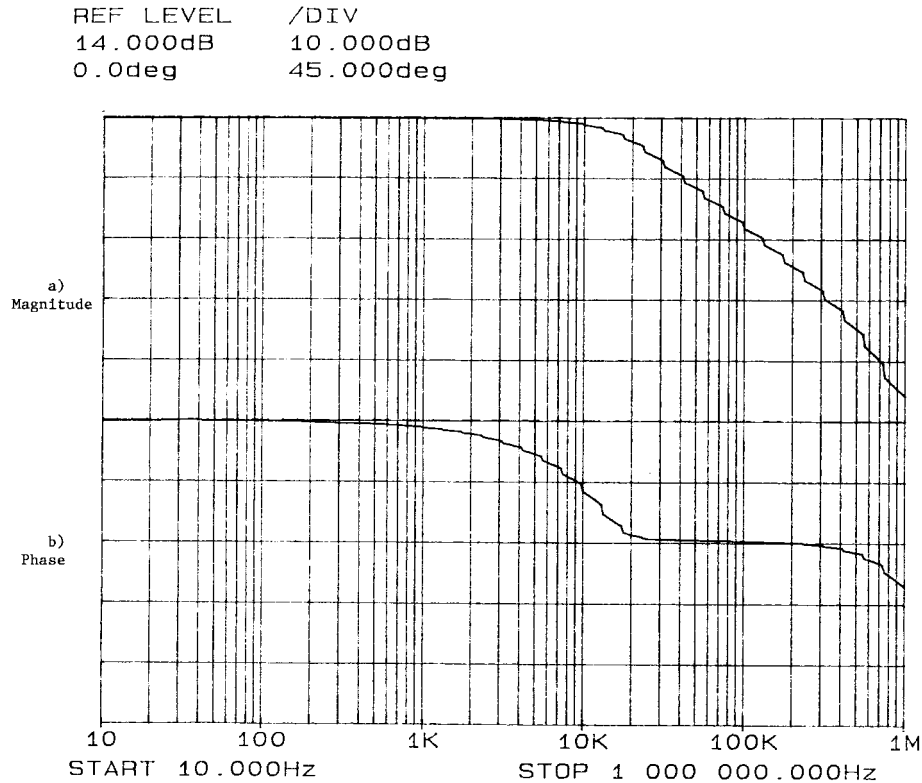


Fig. 4. Experimental results of the integrator using the same values used for the simulation. (a) The magnitude of the voltage transfer function in decibels and (b) the phase of the voltage transfer function in degrees.

For the nonideal case, using (8) with $s = j\omega$, we obtain

$$Q = k \left(\frac{2\omega}{\omega_c} + \omega RC \right). \quad (13)$$

Thus, Q is controllable and it is an increasing function of frequency, k , and the RC product. Thus for $k = 100$, $\omega = \omega_c/2$ and neglecting the term ωRC , $Q \approx 100$. This is to be compared with the traditional differential integrator, with a Q equal to that of the Miller integrator, that has a $Q = -|A| = -|\omega_c/s| = -|\omega_c/\omega|$. Thus, at $\omega = \omega_c/2$, the Miller integrator has a $Q = -2$.

For the ideal or low-frequency case, we obtain the value

$$Q = kRC\omega. \quad (14)$$

Thus, for $RC\omega = 0.1$ and $k = 1000$, we obtain a Q -value of 100.

Thus, for high frequencies, the new integrator could obtain higher values of Q than the traditional integrators. Even at low frequencies, reasonably high Q values could be obtained.

IV. STABILITY

Following the approach of Martin and Sedra [12], a two-pole model is used for the operational amplifier. Let the two poles occur at ω_1 and ω_2 , where ω_1 is the frequency of the first (dominant) pole. Then for $\omega \gg \omega_1$, the open loop gain of the operational amplifier can be expressed as

$$A(s) \approx \frac{\omega_c}{s \left(1 + \frac{s}{\omega_2} \right)}. \quad (15)$$

Substituting (15) into (1), results in the following characteristic equation:

$$q(s) = 2kRCs^3 + (2k\omega_2RC + 2k)s^2 + (2k\omega_2 + \omega_c\omega_2RC + RC\omega_c\omega_2k)s + \omega\omega_2. \quad (16)$$

The Routh–Hurwitz Test tells us that two conditions have to be met to prove that the circuit is stable [13].

- 1) The coefficients of s^i must all have the same sign.
- 2) $a_2a_1 - a_0a_3$ must have the same sign as the coefficients in 1).

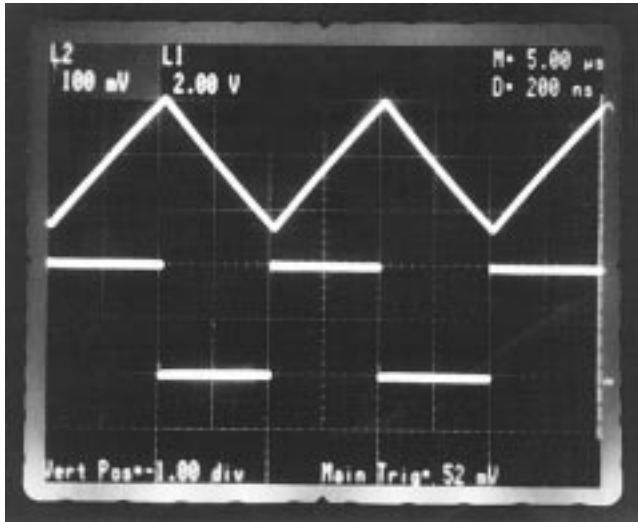
Inspection of $q(s)$ reveals that the first condition is satisfied. Forming the product $a_2a_1 - a_0a_3$ results in

$$a_2a_1 - a_0a_3 = 2k\omega_2(2k\omega_cRC + 2k + R^2C^2\omega_c\omega_2 + kR^2C^2\omega_c\omega_2 + kRC\omega_c). \quad (17)$$

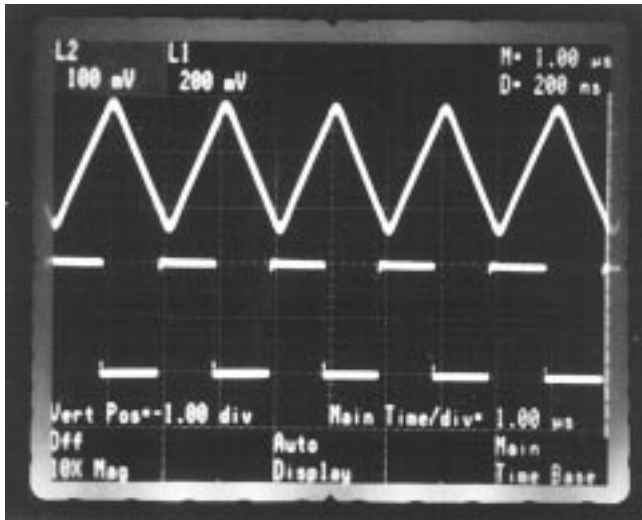
The right-hand side is always greater than zero for $k > 0$ and $\omega_c > 0$. Therefore, the circuit is always stable for $k > 0$ and $\omega_c > 0$.

V. SIMULATION AND EXPERIMENTAL RESULTS

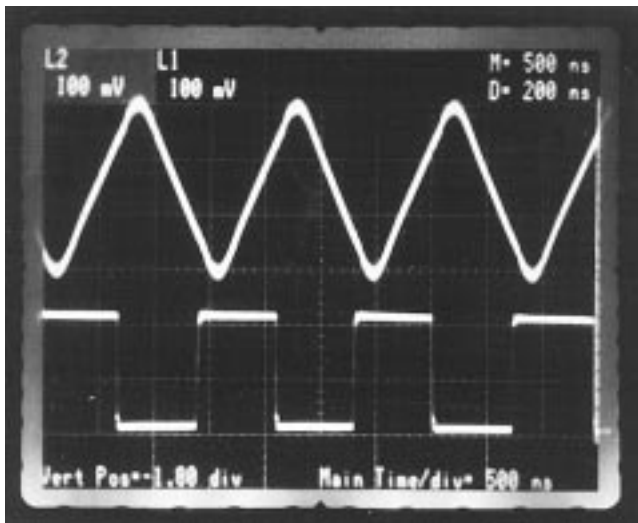
The circuit of Fig. 1 was simulated using HSPICE with $r = 10 \text{ k}\Omega$, $k = 100$, $C = 100 \text{ pF}$, and $R = 500 \text{ }\Omega$ and LM741 for the operational amplifier. The simulation results for the magnitude and phase are shown in Fig. 3. The simulation shows that, with the above values, the circuit acts as an integrator with ten percent phase error from about 35 kHz to over 700 kHz. The same circuit was constructed and tested yielding experimental results close to the simulation



(a)



(b)



(c)

Fig. 5. The triangular waveform responses of the circuit to square waveform inputs at the frequencies (a) 50 kHz, (b) 500 kHz, and (c) 700 kHz.

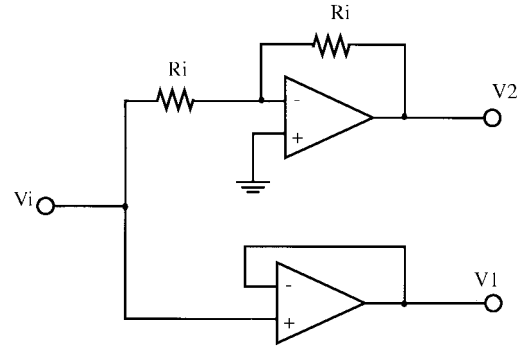


Fig. 6. The experimental setup for obtaining equal voltages of opposite polarities. Both operational amplifiers are LF356 and $R_i = 10\text{ k}\Omega$.

results. The experimental results for the magnitude and phase, using HP3577A Network Analyzer, are shown in Fig. 4 and agree over all with simulation results. The extended frequency range of the integrator is demonstrated by the triangular wave responses to the square wave inputs at frequencies of 50, 500, and 700 kHz as shown in Fig. 5(a)–(c), respectively. The experimental setup, shown in Fig. 6, obtained equal voltages of opposite polarities from the outputs of two LF356 operational amplifiers, one configured as an inverting amplifier with a gain of -1 , and the other as a unity gain voltage follower amplifier. The inputs of the two amplifiers were connected together and the signal applied to the common connection. The output of the inverting amplifier was fed to the input V_2 of Fig. 1 while the output of the voltage follower was fed to V_1 .

The new integrator could be utilized to build resonators with large Q at higher frequencies than those possible by using the traditional Miller integrator. This will be addressed in a subsequent work.

VI. CONCLUSION

A novel stable differential integrator is proposed. It employs a single-time constant and it is also dc stable. It operates at higher frequencies with higher quality factors than the traditional integrators. The usable high-frequency range, due to a built-in high-frequency compensation, could approach the unity gain bandwidth of the employed operational amplifier. Simulation and experimental results verify the theoretical expectations.

APPENDIX

THE DERIVATION OF (1)

In this appendix, the derivation of (1) is outlined. Let V^- , V^+ , and V_R designate the voltages in Fig. 1 from the inverting terminal of the operational amplifier to ground, the noninverting terminal of the operational amplifier to ground and the voltage across the resistor R , respectively.

Nodal analysis at the inverting terminal yields

$$V^- \approx \frac{V_2}{2} + \frac{V_R}{2} + \frac{V_o}{2k}. \quad (A1)$$

The above approximation is obtained by assuming that $k \gg 1$.

Similarly, nodal analysis at the noninverting terminal yields

$$V^+ \approx \frac{V_1}{2}. \quad (\text{A2})$$

Also nodal analysis at the nongrounded terminal of R yields

$$V_R \approx \frac{rRCsV_o + RV^-}{r(1 + RCs)}. \quad (\text{A3})$$

The above approximation is obtained by assuming that $R \ll r$.

Substituting (A3) into (A1), we obtain

$$\begin{aligned} V^- &\approx \frac{V_2}{2} + \frac{RCsV_o}{2(1 + RCs)} + \frac{RV^-}{2r(1 + RCs)} + \frac{V_o}{2k} \\ &\approx \frac{V_2}{2} + \frac{RCsV_o}{2(1 + RCs)} + \frac{V_o}{2k}. \end{aligned} \quad (\text{A4})$$

The above approximation is obtained by assuming that $R \ll r$. Using the equation that relates the voltages at the different terminals of the operational amplifier

$$V_o \approx A(s)(V^+ - V^-) \quad (\text{A5})$$

and substituting the values of V^+ and V^- from (A2) and (A4), respectively, into (A5), we obtain

$$\frac{V_o}{V_1 - V_2} \approx \frac{1}{\frac{2}{A(s)} + RCs + \frac{1}{k}}. \quad (\text{A6})$$

Note that (A6) is the same as (1).

ACKNOWLEDGMENT

The author thanks Professor A. Abidi for providing the atmosphere conducive to research by inviting him to spend the Summer of 1995 at UCLA. He is also grateful to H. Suzuki, P. Pai, E. Roth, B. Harris, A. Liu, D.-S. Park, and M. Wang for their help during his stay at UCLA. Thanks are also due to M. Al-Assir for producing Figs. 1, 2, and 6. It is also a pleasure to acknowledge the outstanding reviewers, whose constructive comments and suggestions contributed considerably to the improvement of the paper.

REFERENCES

- [1] L. P. Huelsman and P. E. Allen, *Introduction to the Theory and Design of Active Filters*. New York: McGraw-Hill, 1980.
- [2] J. G. Graeme, *Designing with Operational Amplifiers: Applications Alternatives*. New York: McGraw-Hill, 1977.

- [3] G. B. Clayton, *Operational Amplifiers*, 2nd ed. Boston, MA: Newnes Butterworth, 1979.
- [4] A. M. Soliman, "Novel generalized differential integrator with controlled phase lead," *Proc. IEEE*, vol. 67, pp. 1449–1451, Oct. 1979.
- [5] R. Schaumann, M. Ghausi, and K. Laker, *Design of Analog Filters*. Englewood Cliffs, NJ: Prentice-Hall, 1990.
- [6] S. Franco, *Design with Operational Amplifiers and Analog Integrated Circuits*. New York: McGraw-Hill, 1988.
- [7] M. A. Al-Alaoui, "A novel approach to designing a noninverting integrator with built-in low frequency stability, high frequency compensation and high Q ," *IEEE Trans. Instrum. Meas.*, vol. 38, pp. 1116–1121, Dec. 1989.
- [8] R. L. Geiger and G. R. Bailey, "Integrator design for high-frequency active filter applications," *IEEE Trans. Circuits Syst.*, vol. CAS-29, pp. 595–603, Sept. 1982.
- [9] J. G. Graeme, G. E. Tobey, and L. P. Huelsman, Eds., *Operational Amplifiers, Design and Applications*. Tokyo, Japan: McGraw-Hill, Kogakusha, 1971.
- [10] P. E. Allen and W. J. Parrish, "High frequency response of inverting integrators," *IEEE J. Solid-State Circuits*, vol. SC-11, pp. 545–547, Aug. 1976.
- [11] J. R. Brand and R. Schaumann, "Active R filters: Review of theory and practice," *IEE J. Elect. Circuits Syst.*, vol. 2, pp. 89–101, July 1978.
- [12] K. Martin and A. S. Sedra, "On the stability of phase-lead integrator," *IEEE Trans. Circuits Syst.*, vol. CAS-24, pp. 321–324, June 1971.
- [13] R. C. Dorf, *Modern Control Systems*, 6th ed. Reading, MA: Addison-Wesley, 1993, pp. 211–214.



Mohamad Adnan Al-Alaoui (S'70–M'83–SM'91) received the B.S. degree in mathematics from Eastern Michigan University, Ypsilanti, in 1963, the B.S.E.E. degree from Wayne State University, Detroit, MI, in 1965, and the M.S.E.E. and Ph.D. degrees in electrical engineering from the Georgia Institute of Technology, Atlanta, in 1968 and 1974, respectively.

From 1966 to 1967, he served as an Assistant Project Engineer in the Avionics Departmentm Bendix Radio Divisionm Baltimore, MD. From 1968 to 1974, he held teaching assistant positions at the School of Electrical Engineering and the School of Mathematics, Georgia Institute of Technology. In 1976, he joined the Electrical Engineering Department at Royal Scientific Society, Amman, Jordan, where he was responsible for the communications area. He served as an Assistant Professor in the EE Department at the American University of Beirut, Lebanon, from 1977 to 1980. He was a visiting Assistant and Associate Professor at the EECs Department, University of Connecticut, Storrs, from 1980 to 1982 and in the Summer of 1985. He served as an Associate Professor of Electrical Engineering at the Hartford Graduate Center, Hartford, CT, from 1983 to 1985. He was the Chairman of the Automatic Control Department at the Higher Institute for Applied Science and Technology, Damascus, Syria, from 1985 to 1988. In 1988, he rejoined the American University of Beirut, where he is currently a Professor of Electrical and Computer Engineering. His research interests are in neural networks and their applications in instrumentation, communications, and controls.

Dr. Al-Alaoui was awarded the First Research Award in Engineering for 1989–1990 by the American University of Beirut.